The Journal of Experimental Biology 201, 913–923 (1998)
Printed in Great Britain © The Company of Biologists Limited 1998
JEB1184

SCALING OF MUSCLE PERFORMANCE DURING ESCAPE RESPONSES IN THE FISH *MYOXOCEPHALUS SCORPIUS* L.

ROB S. JAMES* AND IAN A. JOHNSTON

Gatty Marine Laboratory, School of Environmental and Evolutionary Biology, University of St Andrews, St Andrews, Fife KY16 8LB, Scotland, UK

*e-mail: rsj@st-and.ac.uk

Accepted 20 January; published on WWW 5 March 1998

Summary

Fast-starts associated with escape responses were studied in short-horn sculpin (*Myoxocephalus scorpius* L.), ranging from 5.5 to 32 cm in total length (*L*). Electromyography and sonomicrometry were used simultaneously to measure muscle activation and length changes, respectively, in the superficial layers of fast muscle in rostral myotomes. Escape responses consisted of a half tailbeat to bend the body into a C-shape (C-bend), another half tailbeat (contralateral contraction), followed by one or two more tailbeats and/or a gliding phase. The scaling relationships for both muscle strain and shortening duration differed between the C-bend and the contralateral contraction. As a result, relative muscle shortening velocity (V/V_0) scaled as $-1.18L^{1.06}$ for the C-bend and as $1.23L^{-0.66}$ for the contralateral contraction. Therefore, the scaling relationships for muscle shortening velocity varied throughout the time course of the escape response. Muscle power output was determined by using the work-loop technique to subject isolated muscle fibres to *in vivo* strain and stimulation patterns. Plots of the instantaneous muscle forces and velocities achieved during the contralateral contraction were found to deviate from the steady-state force–velocity relationship. Maximum instantaneous muscle power output was independent of body size, with mean maximum values of 307 and 222 W kg^{-1} wet muscle mass for the C-bend and the contralateral contraction, respectively.

Key words: electromyography, escape response, fish, kinematics, mechanics, *Myoxocephalus scorpius*, scaling, short-horn sculpin, sonomicrometry.

Introduction

To escape from predators, fish use rapid, carefully timed and directed movements which involve the recruitment of the entire white muscle (for a review, see Domenici and Blake, 1997). Although escape responses are continuous events, they have often been classified into distinct kinematic stages (Weihs, 1973; Webb, 1978). Initially, the body of the fish is bent into a ‘C’ or ‘S’ shape, rapidly rotating the head so as not to provide a stationary target (Eaton *et al.* 1977). The C-bend is then followed by one or more complete tailbeats of variable amplitude and duration which usually involve an overall change in direction (see Domenici and Blake, 1997). Length-specific swimming velocity decreases with increasing body length (Videler and Wardle, 1991; Gibson and Johnston, 1995), whereas tailbeat duration increases (Bainbridge, 1958; Webb, 1978). The scaling of kinematic parameters has been attributed to systematic variations in the mechanical properties of muscle (Wardle, 1980). For example, James *et al.* (1998) found that in short-horn sculpin (*Myoxocephalus scorpius* L.) the activation and relaxation times of muscle increased and the maximum unloaded shortening velocity (V_0) decreased with increasing body length.

Johnston *et al.* (1995) studied muscle performance during predation fast-starts in the short-horn sculpin. Successive outlines of the body were digitised and used together with a knowledge of the geometric arrangement of muscle fibres to calculate *in vivo* muscle strain changes. In order to estimate *in vivo* muscle power output, an adaptation of the work-loop technique (Josephson, 1985; Altringham and Johnston, 1990) was used to measure power output *in vitro* in fibre bundles subjected to the calculated strain waveforms and measured *in vivo* muscle activation patterns. In addition, instantaneous force was plotted against velocity to produce a power loop (Stevens, 1993), allowing comparisons of muscle performance under *in vivo* and steady-state (isovelocity) conditions. The amount of active lengthening of the muscle prior to shortening (pre-stretch) was found to increase down the length of the fish, resulting in a progressive increase in the amount of force enhancement. Pre-stretch caused the muscle properties to deviate from those found under steady-state conditions such that higher V/V_{max} (shortening velocity expressed as a proportion of maximum shortening velocity) values were used *in vivo* than would have been predicted from force–velocity curves.

The aim of the present study was to investigate the scaling

of *in vivo* muscle performance during fast-starts associated with escape responses in the short-horn sculpin. The approach used was an advance on that used by Johnston *et al.* (1995) in that direct measurements of muscle strain were made using sonomicrometry synchronised with electromyographical recordings.

Materials and methods

Short-horn sculpin (*Myoxocephalus scorpius* L.) were caught by local fishermen in the Firth of Forth, Scotland. Twenty-nine fish were acclimated to 12 °C for 5–7 weeks (12 h:12 h light:dark photoperiod) in recirculating seawater tanks (1.0 m×0.51 m: diameter × depth). Fish were fed on shrimp (*Crangon crangon*) and chopped squid.

Muscle fibre geometry

Preliminary studies of the orientation of myotomal muscle fibres were undertaken to determine a region in which fast muscle fibres were aligned parallel to the skin in both the horizontal and vertical planes. Two fish of 20.3 cm and 25.5 cm total length were killed by a blow to the head and pithing, and allowed to go into rigor. Sections of skin and muscle were taken as longitudinal vertical or longitudinal horizontal sections through the fish. Sections of muscle were inspected under a dissecting microscope to determine the alignment of fast muscle fibres with respect to the median and frontal planes of the fish, as described by Alexander (1969).

In rostral myotomes, the muscle fibres ran parallel to the skin for up to 2 mm depth in the medial plane and up to 0.9 mm depth in the frontal plane.

Implantation of electromyography wires and sonomicrometry crystals

Eighteen fish (ranging from 17 to 32 cm total body length, 79–550 g body mass) were anaesthetised using a 1:5000 (m/v) solution of tricaine methanesulphonate (MS222) containing 0.70 mmol l^{-1} sodium hydrogen carbonate. Anaesthesia was maintained during surgery by irrigation of the gills with a 1:7000 (m/v) concentration of MS222. The surgical methods and the sonomicrometry and electromyography techniques used to measure muscle length changes and activation patterns were based on those of Franklin and Johnston (1997).

Electromyography (EMG) electrodes were constructed from two lengths of 150 μm diameter Teflon-coated silver wire (A-M Systems, Everett, USA) with 2 mm of insulation removed from both ends of the wires. EMG wires were implanted directly through the skin into the muscle through a hole made using a 21 gauge syringe needle. EMG wires were implanted 2–4 mm medial to the midpoint between the sonomicrometry crystals (see below) at a depth of 1–1.5 mm below the skin. EMG recordings were amplified using a differential a.c. amplifier (AM Systems, Everett, USA) with low and high cut-off settings of 100 Hz and 5000 Hz, respectively.

A small square of Perspex (2 mm×2 mm×0.5 mm) was attached to the wire 1–1.5 mm behind each sonomicrometry crystal (1 mm diameter, lensed crystal, Triton Technology Inc., San Diego, USA). A small incision was made in the skin on the dorsal surface of the fish, and a hole was made in the exposed rostral muscle using a 19 gauge syringe needle. Sonomicrometry crystals were implanted into holes made as described, with 8–12 mm (1–2 myotomes) between the emitter and receiver crystal, at a distance of 0.35 total body lengths (*L*) from the snout of the fish. An oscilloscope was connected to the sonomicrometer circuit to check the alignment of the pair of sonomicrometry crystals. The square Perspex implants on the surface of the myotome helped to maintain crystal alignment by ensuring that each of a pair of sonomicrometry crystals was implanted to the same depth. A correction of 5 ms was used for the lag in sonomicrometry readings due to the data filter in the Triton Technology model 120 sonomicrometer. We calculated that the errors in sonomicrometry readings due to the change in the velocity of sound through the crystal lens and to the changes in muscle stiffness (Tamura *et al.* 1982) were less than 4 % of the measured strain. Crystal rotation of 30 ° or more is known to cause problems in the triggering of the sonomicrometer (Kirkpatrick *et al.* 1973), resulting in extremely rapid changes in output. Such problems were extremely rare and any traces showing these symptoms were discarded. Therefore, errors due to crystal rotation should have been less than 2 % of the measured strain.

The incisions made in the skin for sonomicrometry crystal implantation were sutured and all exposed wires were sutured externally to the skin, allowing some slack to avoid rapid movements by the fish from dislodging the crystals or wire. Fish were allowed to recover overnight and swimming experiments were performed over the following 2–3 days. After they had been killed, X-rays of dorsal and lateral views of the first two fish were used to confirm the positions of the implanted sonomicrometry crystals and EMG wires. In most fish, the rostral muscle was also dissected to confirm placement of crystals/electrodes and to detect any local damage caused by the surgical and experimental procedures. Damage to the muscle appeared to be minimal and was assumed to have no influence on local muscle strain. The total mass of two pairs of sonomicrometry crystals and wires and two EMG wires was less than 8 g. The smallest fish in which sonomicrometry crystals could be implanted successfully was 17 cm total length.

Escape behaviour and in vivo *muscle properties*

Fish with (*N*=18) and without (*N*=11) EMG wires and sonomicrometry crystals (ranging from 5.5 to 32 cm *L*, 1.9–550 g body mass) were filmed in a static tank (2.0 m×0.62 m×0.26 m, length × width × depth) of circulating sea water maintained at 12 °C. The tank had a Perspex base and was lit from underneath by five 70 W fluorescent strip lights.

Escape responses were elicited by touching the tail of the fish with a metal rod presented from behind the fish at an angle of 30–45 ° to the midline of the tail. The resultant escape response was filmed in silhouette from above using a mirror angled at 45 ° to a high-speed ciné camera (NAC, Japan) operating at 500 frames s^{-1}.

Ciné films of fish and EMG and sonomicrometry recordings were synchronised using a pulsed light source in the filming arena. EMG and sonomicrometry recordings were used to monitor *in vivo* muscle activation and length changes (strain), respectively (Franklin and Johnston, 1997). The error in matching a frame of ciné film to the sonomicrometry and electromyography data was estimated to be less than 2 ms.

Initial observations demonstrated that *in vivo* muscle velocity was relatively constant throughout the majority of the shortening period of the strain records. Therefore, shortening velocity (V) was calculated as the slope of the tangent fitted to the region of strain data with relatively constant shortening velocity. James *et al.* (1998) used the slack test method to measure the maximum unloaded shortening velocity (V_0) over a larger body size range of short-horn sculpin than used in the present study. In the present study, V_0 was calculated for each fish using the scaling exponent of $19.5L^{-0.34}$ from James *et al.* (1998). V/V_0 was then calculated for *in vivo* strain data from each fish.

Kinematic analysis

The position of the snout and centre of mass (see below) of each fish was digitised for each frame of ciné film using a motion-analysis system (MOVIAS, NAC, Japan). An object of known length was digitised on the first frame of each escape response sequence to act as a distance calibration. Errors in digitising the snout and centre of mass caused an error of less than ±1.5 % in both the x and y position coordinates. The smoothed position data were interpolated from the best-fit least-squares cubic regression line fitted to that data point and the adjacent 20 points**.** The smoothed position data were used to calculate the velocity (U) of the fish. For each fish, only the sequence with the highest maximum velocity (U_{max}) of the centre of mass was selected for further analysis.

Outlines of the fish were traced for the beginning of the escape response, the end of the C-bend and the end of the contralateral contraction. The end of the C-bend was taken to be the time when the fish had reached the end of the first half tailbeat (most extreme tail position). The end of the contralateral contraction was determined to be the time when the fish had finished another half tailbeat after the initial C-bend. The tailbeat amplitude was determined as the total lateral distance the tail had moved during the C-bend and the contralateral contraction. The stride length was calculated as the straight-line distance moved from the beginning of the response to the end of the contralateral contraction. The turning angle was calculated using MOVIAS by drawing a line from the snout to the centre of mass of the fish and measuring the angle of rotation during the C-bend. The position of the centre of mass was determined using the methods of Temple and Johnston (1998).

Work-loop experiments

In vitro studies on the contractile properties of muscle were performed as outlined by James *et al.* (1998). Fish (N=9) were stunned by a blow to the head and pithed to destroy the central nervous system. Small bundles of 6–20 fibres were dissected from anterior abdominal myotomes in Ringer's solution maintained at 4 °C. The Ringer's solution contained (in mmol l^{-1}): NaCl, 143; sodium pyruvate, 10; KCl, 2.6; $MgCl_2$, 1.0; $NaHCO_3$, 6.18; NaH_2PO_4, 3.2; $CaCl_2$, 2.6; Hepes sodium salt, 3.2; Hepes, 0.97. An aluminium foil T-shaped clip was folded over the myoseptum at each end of the muscle fibre bundle preparation. The preparation was then transferred to a flow-through chamber of Ringer maintained at 12 °C. The foil clips were used to attach the preparation to a force transducer at one end (AME 801, SensoNor, Norway) and a servo arm at the other. Muscle fibre preparations were initially held at constant length. Stimulus amplitude (8–15 V), pulse width (0.8–1.5 ms) and fibre length were adjusted to maximise twitch force. The muscle fibre length that maximised twitch force was termed L_0 and corresponded to a length of 9.2±0.7 mm (mean ± S.E.M.). Stimulation frequency was adjusted to maximise tetanus height (80–140 Hz). Muscle preparations were then used for work-loop studies.

In order to produce the cyclical events needed for work-loop experiments, segments of representative strain records corresponding to the C-bend and the contralateral contraction were abstracted. The abstracted strain waveforms for both the C-bend and the contralateral contraction began at the start of the escape response and continued until the muscle had undergone shortening and returned to its initial length. The abstracted *in vivo* muscle strain waveforms were digitised then smoothed. The smoothing procedure estimated the value of each point by fitting a best-fit least-squares cubic regression to approximately 10 % of the data. Instantaneous strain rate was calculated from the smoothed muscle strain data. For 10 fish that had been used for studies of isometric contractile properties (James *et al.* 1998; 17–30 cm total body length, 79–461 g body mass), the isolated muscle preparations were subjected to the abstracted strain waveforms and stimulated at the appropriate point in the strain cycle and for the same duration as found *in vivo*. The results for both the C-bend and the contralateral contraction have nine replicates as two of the fish used had both electromyography and sonomicrometry results for only one side of the fish. On completion of the *in vitro* mechanical experiments, the cross-sectional area and wet mass of each muscle preparation were calculated as outlined by James *et al.* (1998).

Statistics

Unless stated otherwise, all values are means ± S.E.M. (N is the number of observations). Unpaired, two-sided t-tests were used to make statistical comparisons between sets of data. Each regression line represents a first-order polynomial fitted to each set of log–log data using a least-squares regression. The values for the scaling exponents (in the form $aL^{b\pm SE}$, where a represents the intercept at unity, b represents the slope of the regression line and SE represents the standard error of the slope) and the correlation coefficient (r^2) are given for each regression line. Data presented as percentages were converted to proportions and arcsine-transformed prior to calculating the mean and S.E.M. The mean and S.E.M. of arcsine-transformed data were then back-transformed with the S.E.M. being presented as a range of values.

For figures with more than one regression line, the slopes and elevations of each pair of lines were compared using the relevant *t*-tests (Zar, 1984). The use of the term 'significant' in the text signifies a *P* value of less than 0.05.

Results

Kinematics

Kinematic parameters were determined for the 11 unwired fish and 13 of the wired fish (those with sonomicrometry and EMG wires implanted). The results for the wired fish all fell within the confidence intervals of the results from the unwired fish. All kinematic data from wired and unwired fish were subsequently pooled for further analysis.

As total body length (L) increased, the maximum length-specific swimming velocity decreased significantly for both the snout and the centre of mass during both the C-bend and the contralateral contraction (Fig. 1A,B). The slopes of the regression lines fitted to the data for maximum length-specific velocity ($\bar{U}_{max}$) of the snout were significantly different between the C-bend and the contralateral contraction (Fig. 1A). This difference was due to a disproportionate increase, with increased body length, in the absolute maximum velocity (U_{max}) and therefore a disproportionate decrease in $\bar{U}_{max}$ achieved by the snout during the C-bend compared with the contralateral contraction (Figs 1A, 2).

Stride length and duration of the C-bend and the contralateral contraction all increased significantly with increasing body length (Table 1). The turning angle during the C-bend increased significantly with body length, ranging from 25.8 to 127 °, whereas the total tailbeat amplitude used during the C-bend and contralateral contraction showed no clear trend with changing body size and was highly variable, ranging from 0.3 to 1.2L (Fig. 3). U_{max} increased significantly with increasing body length (Table 1) ranging from 0.52 to 2.24 m s^{-1} and from 0.45 to 1.61 m s^{-1} for the snout and the centre of mass, respectively.

Electromyography and sonomicrometry

In this study, irregular strain waveforms were observed throughout all escape responses in contrast to the repetitive near-sinusoidal strain waveforms determined previously for steady swimming in a range of fish species (for a review, see Wardle *et al.* 1995). During the C-bend, muscle on one side of the fish was activated and subsequently underwent shortening, with activation being terminated before the shortest muscle length was reached (Fig. 4, green trace). Muscle on the opposite side of the fish lengthened prior to activation, then continued to lengthen before shortening actively during the contralateral contraction of the tail (Fig. 4, red trace). In a few fish, wires were successfully implanted in only one side of the fish; hence, the numbers of replicates for the C-bend and contralateral sides are lower than the number of fish used.

The shortening duration of rostral muscle fibres increased significantly with increasing body length, scaling as $L^{1.42}$ and $L^{1.60}$ for the C-bend and the contralateral contraction, respectively (Fig. 5A; Table 2). The slopes of the regression lines for shortening duration during the C-bend and the contralateral contraction were not significantly different from each other (P>0.10), but the elevations of the lines did differ significantly (P<0.05).

The total muscle strain during shortening increased significantly with an increase in total body length, scaling as $L^{2.41}$ and $L^{1.08}$, respectively, for the C-bend and the contralateral contraction, with the slopes of these regression

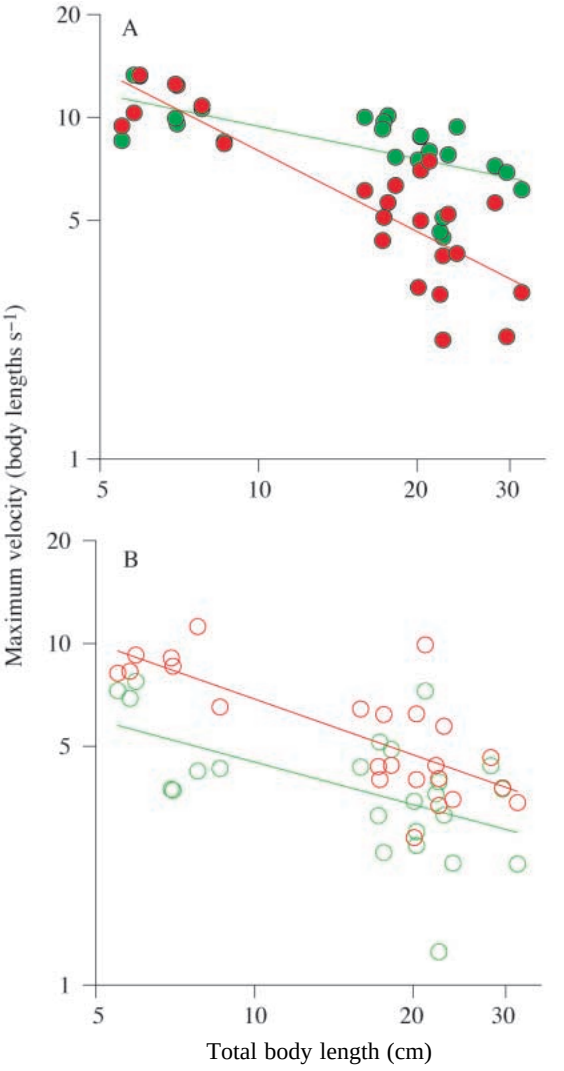

Fig. 1. Changes in maximum length-specific swimming velocity ($\bar{U}_{max}$) of the snout (A) and the centre of mass (B) with increasing body length. Each line represents a first-order polynomial fitted to a set of log–log data using a least-squares regression. Green and red traces represent the C-bend and the contralateral contraction, respectively. During the C-bend, the scaling relationships for the snout and centre of mass were $19.5\pm1.25L^{-0.32\pm0.08}$ (r^2=0.41, P<0.001) and $48.9\pm1.35L^{-0.79\pm0.11}$ (r^2=0.71, P<0.001), respectively, where L is total body length (N=24). During the contralateral contraction, the scaling relationships for the snout and the centre of mass were $11.6\pm1.45L^{-0.41\pm0.13}$ (r^2=0.71, P<0.001) and $24.0\pm1.32L^{-0.54\pm0.10}$ (r^2=0.58, P<0.001).

The total muscle strain during shortening increased significantly with an increase in total body length, scaling as $L^{2.41}$ and $L^{1.08}$, respectively, for the C-bend and the contralateral contraction, with the slopes of these regression

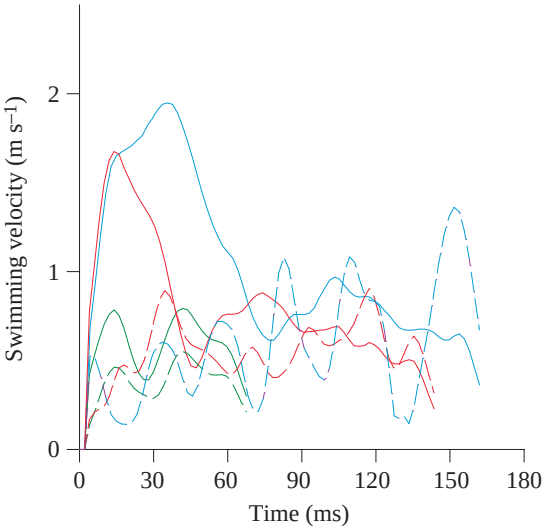

Fig. 2. Changes in swimming velocity (U) over time for three fish differing in body length. Solid lines and broken lines represent the velocity of the snout and velocity of the centre of mass, respectively. Blue, red and green data represent fish of 31.6, 17.3 and 6.0 cm total body length, respectively.

lines being significantly different (P<0.05, Fig. 5B; Table 2). During the C-bend, muscle shortening velocity increased significantly with increasing total body length, scaling as $L^{1.06}$, because the increase in muscle strain was only partially matched by the rise in shortening duration (Fig. 5C; Table 2). However, the shortening velocity during the contralateral contraction decreased significantly with an increase in fish total body length, scaling as $L^{-0.66}$, a significantly different slope from that found during the C-bend (P<0.01), as the rise in shortening duration with increased total body length was not matched by a comparable rise in strain.

V/V_0 for the C-bend increased with increasing fish total length ranging from 0.15 to 0.38, scaling as $L^{1.37}$ (Fig. 5D; Table 2). During the contralateral contraction, muscles shortened at approximately $0.30V/V_0$ irrespective of body length, with a range of 0.22–0.40 (Fig. 5D). The slope of the regression line fitted to the V/V_0 data was significantly different between the C-bend and the contralateral contraction (P<0.01).

Work-loop experiments

The muscle stress generated varied throughout the simulated escape response (Fig. 6A–F). Muscle stress initially increased during shortening as the activation level of the muscle increased. The maximum stress achieved was lower during the C-bend than the contralateral contraction, reaching $0.71\pm0.04P_{max}$ (mean ± S.E.M.), where P_{max} is the maximum isometric force, compared with $0.95\pm0.04P_{max}$, respectively (Fig. 6E,F). The stress generated during the contralateral contraction approached, and in a few fish actually exceeded, the maximum stress achieved under isometric contractions (where the mean P_{max} was 198±9.7 kN m^{-2}).

The instantaneous muscle power output (i.e. force × velocity) produced during the C-bend was largely positive (i.e. the muscle was producing work, Fig. 6G,H). In contrast, during the initial stages of the contralateral contraction, there was a substantial amount of negative power output (work was done upon the muscle) due to the period of active muscle lengthening prior to shortening. During the C-bend, the mean maximum instantaneous power output was significantly lower than that achieved during the contralateral contraction, 222

Table 1. *The effects of body length on various kinematic parameters of the escape response*

		Length-specific scaling relationship			
	Units	log$a$	b	r^2	P
C-bend duration	ms	1.03±0.12	0.54±0.10	0.59	<0.001
Contralateral contraction duration	ms	1.35±0.09	0.58±0.07	0.74	<0.001
Stride length	cm	–0.59±0.20	1.12±0.17	0.67	<0.001
Turning angle during the C-bend	degrees	1.14±0.16	0.48±0.13	0.38	<0.01
Total tailbeat amplitude used during the C-bend and contralateral contraction	L	–0.08±0.14	–0.10±0.11	0.03	0.39
Maximum absolute velocity (U_{max}) of the snout	m s^{-1}	–0.63±0.08	0.63±0.07	0.79	<0.001
Maximum absolute velocity (U_{max}) of the centre of mass	m s^{-1}	–0.62±0.09	0.47±0.09	0.65	<0.001
Maximum length-specific velocity ($\bar{U}_{max}$) of the snout	L s^{-1}	1.37±0.08	–0.36±0.07	0.54	<0.001
Maximum length-specific velocity ($\bar{U}_{max}$) of the centre of mass	L s^{-1}	1.37±0.09	–0.53±0.07	0.71	<0.001

Values represent the scaling relationship expressed as aL^b (where a is the intercept at unity ± S.E.M., L is the total body length of the fish in cm and b is the slope of the regression line ± S.E.M.) and the correlation coefficient (r^2) value.

Twenty-four fish were used.

Each velocity value represents the maximum velocity achieved during the escape response.

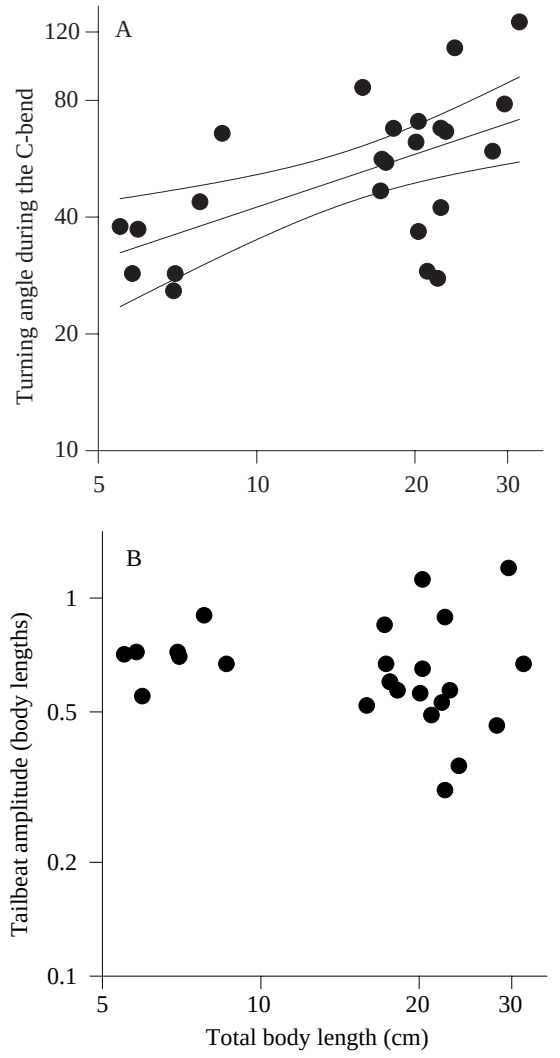

Fig. 3. The effects of increasing total body length on (A) turning angle used during the C-bend and (B) total tailbeat amplitude used during the C-bend and contralateral contraction. The lines represent a first-order polynomial fitted to the log–log data using a least-squares regression and the 95 % confidence intervals for each regression line. The scaling relationships are given in Table 1.

compared with 307 W kg^{-1} wet muscle mass, respectively (Table 3). Maximum instantaneous power output was independent of body length during both the C-bend and the contralateral contraction.

The mean power output produced during the abstracted cycle was very similar for the C-bend and the contralateral contraction, being 41.7±7.3 and 41.0±5.0 W kg^{-1} wet muscle mass (mean ± S.E.M.), respectively. The mean power output increased significantly with body length during the C-bend, scaling to $0.03L^{2.31\pm0.20}$ (r^2=0.54, P<0.05), but was independent of body length during the contralateral contraction.

When stimulus timing, stimulus duration, strain or strain duration was altered individually whilst maintaining the other parameters at their *in vivo* values, mean power output improved on average by between 2 and 14 %. For the contralateral contraction, each parameter when altered improved mean power output by mean values of between 6 and 20 %. The muscle fibres studied delivered closer to their maximum power output during the contralateral contraction than during the C-bend of the escape response.

When the strain and stimulation patterns measured during the C-bend were imposed on isolated muscle, the forces achieved at certain velocities approached, but never exceeded, the force–velocity relationship determined under isovelocity conditions (Fig. 7). However, when the strain and stimulation patterns measured during the contralateral contraction were imposed on isolated muscle, higher forces were achieved at certain shortening velocities than would have been predicted from steady-state force–velocity curves. At the onset of shortening, muscle velocity increased dramatically at near-constant load ($0.85P_{max}$ in Fig. 7B).

Discussion

Changes in swimming strategy with body size

Escape behaviour changed with increases in body size. Significantly greater turning angles were used during the C-bend, scaling as $L^{0.48}$ (Fig. 3A; Table 1), whereas length-specific tailbeat amplitude during the C-bend and the contralateral contraction did not change (Fig. 3B; Table 1). A

Table 2. In vivo *muscle strain parameters during escape responses*

		Length-specific scaling relationship							
		C-bend				Contralateral contraction			
	Units	log*a*	*b*	r^2	*P*	log*a*	*b*	r^2	*P*
Shortening duration	ms	–0.17±0.49	1.42±0.35	0.53	<0.01	–0.26±0.76	1.60±0.56	0.37	<0.05
Strain		–4.40±0.62	2.41±0.45	0.67	<0.001	–2.40±0.45	1.08±0.33	0.43	<0.01
Shortening velocity (*V*)	muscle lengths s^{-1}	–1.18±0.28	1.06±0.20	0.67	<0.001	1.23±0.30	–0.66±0.22	0.40	<0.01
V/V_0		–2.42±0.28	1.37±0.20	0.76	<0.001	–0.56±0.38	0.03±0.28	0.001	>0.9

Shortening velocity (*V*) was calculated by fitting a tangent to the strain data.

Values represent the scaling exponents (in the form aL^b, where *a* represents the intercept at unity ± S.E.M. and *b* represents the slope of the regression line ± S.E.M. and *L* is total body length) and the correlation coefficient (r^2) for 16 fish.

V_0 represents maximum unloaded shortening velocity calculated for each fish using the scaling equation from James *et al.* (1998).

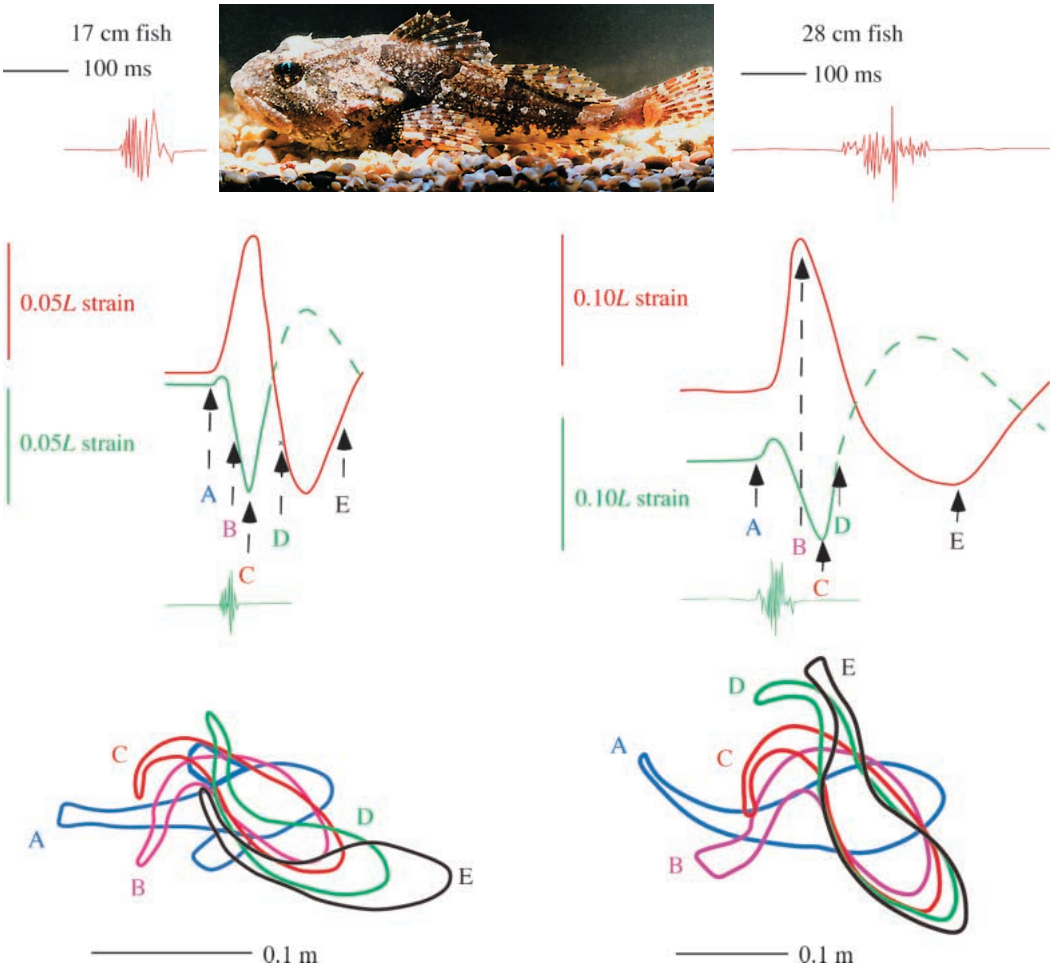

Fig. 4. *In vivo* recordings of muscle strain (central panels) and activity patterns (upper panels) collected during an escape response for fish of 17 cm and 28 cm total body length. A strain of 0.10*L* refers to a 10 % change in muscle length with respect to initial resting length. Outlines of fish (lower panels) were digitised from high-speed films taken at 500 frames s^{-1}. Red and green traces denote electromyography and sonomicrometry data for rostral muscle on opposite sides of the fish. The solid part of the lines indicates the abstracted strain waveforms used subsequently for *in vitro* studies. The photograph shows the external morphology of a short-horn sculpin of 20 cm total length.

larger turning angle represents an increase in the movement of the head, which is usually the prime target for predators, resulting in a relatively higher velocity of the snout during the C-bend (Figs 1, 2). The reasons for differences in swimming kinematics observed between different sizes of fish are unknown.

Muscle shortening and tailbeat durations

During both the C-bend and the contralateral contraction of the escape response, a wave of bending travels down the length of the fish. If the relative muscle shortening period along the length of the fish is constant with increases in body size, then the scaling exponents of tailbeat duration and rostral muscle shortening duration will be the same, i.e. the wave of muscular contraction will travel down the body at the same rate as the wave of bending. The rostral muscle shortening duration increased significantly with body length, scaling as $L^{1.42}$ and $L^{1.60}$ for the C-bend and the contralateral contraction, respectively (Fig. 5A; Table 2). In contrast, tailbeat duration scaled as $L^{0.54}$ and $L^{0.58}$ for the C-bend and the contralateral

Table 3. *Results from work-loop experiments*

	C-bend			Contralateral contraction		
	Mean	Range of S.E.M.	Range of values	Mean	Range of S.E.M.	Range of values
Mean power output (W kg^{-1} wet muscle mass)	41.7	34.5–49.0	11.0–72.7	41.0	36.0–46.0	18.0–64.7
Maximum instantaneous power output (W kg^{-1} wet muscle mass)	222*	201–243	125–322	307	287–327	202–401

Muscle power output produced at 12 °C during the simulated C-bend and contralateral contraction of the escape response.
Values are for nine fish ranging from 17 to 30 cm total body length.
*Represents a significant difference (P<0.05) between the mean values for the C-bend and the contralateral contraction.

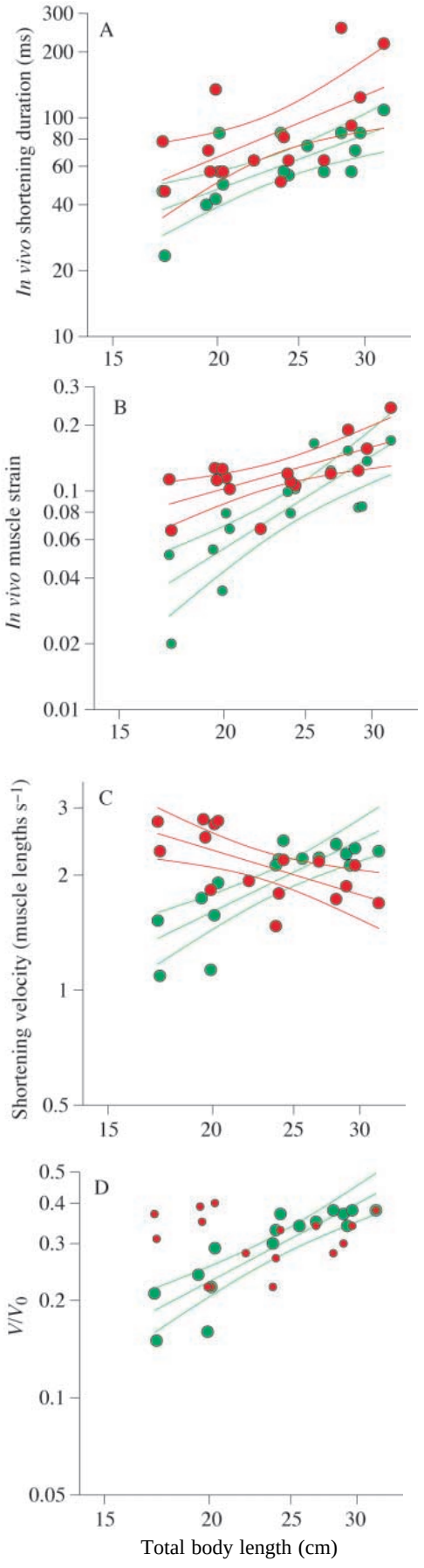

contraction, respectively (Table 1). The signs for the scaling exponents of tailbeat duration and muscle shortening duration *in vivo* are the same, but their magnitudes are significantly different. Therefore, the wave of muscle shortening travels down the body at a different rate from the wave of bending.

Jayne and Lauder (1993, 1995) found that during the C-bend the EMG onset time is almost instantaneous along the length of fish. This finding suggests that, for a wave of muscle shortening to occur in short-horn sculpin, there must be a change in the properties of fast muscle fibres along the length of the fish. Indeed, James *et al.* (1998) found that muscle activation rate, relaxation rate and maximum shortening velocity (V_{max}) were consistently faster in rostral than caudal myotomes, although the differences were only significantly different for V_{max}. Jayne and Lauder (1993) found that during the contralateral contraction the EMG onset time propagated posteriorly but at a more rapid rate than did the wave of bending. Again, the wave of muscle bending is likely to be due to the increase in muscle activation and relaxation times along the length of the fish.

Scaling of V/V$_{max}$

The relationship between *in vivo* muscle shortening velocity and *in vitro* maximum shortening velocity (V/V_{max} ratio) gives an indication of the force and power that are likely to be produced by a muscle at a given time. The V/V_0 ratio (where V_0 is the maximum unloaded shortening velocity determined using the slack test method) of 0.28 used during the contralateral contraction equates to a V/V_{max} ratio of 0.31 (as V_{max} in the sculpin is $0.9V_0$ at 12 °C; R. S. James and I. A. Johnston, unpublished results). The value of 0.31 for V/V_{max} is comparable to the V/V_{max} of 0.29 calculated previously for 22 cm total length short-horn sculpin during prey capture (Johnston *et al.* 1995) and is within the V/V_{max} range for maximum power output determined from the force–velocity (*P*–*V*) curve (R. S. James and I. A. Johnston, unpublished results; Curtin and Woledge, 1988; Rome and Sosnicki, 1990). Studies on frog jumping have also found that fast muscle used primarily for the production of high power output operates at a V/V_{max} value close to 0.3 (Lutz and Rome, 1994). The V/V_0 ratio of 0.17–0.42 used during the C-bend increased with increasing body length such that the values used equated to a V/V_{max} range which, according to steady-state force–velocity studies, should yield more than 88 % of maximum power

Fig. 5. The effects of fish body length on muscle performance during escape responses. (A) Shortening duration, (B) strain, (C) shortening velocity calculated by fitting a tangent to the strain data, (D) shortening velocity/maximum shortening velocity calculated using the slack-test method (V/V_0). Data represent the maximal escape response recorded for each fish, determined as the response with the highest muscle shortening velocity (N=16). Green and red traces represent the C-bend and the contralateral contraction, respectively. The lines represent a first-order polynomial fitted to the log–log data using a least-squares regression and the 95 % confidence intervals for each regression line.

output. This is similar to the V/V_{max} range of 0.18–0.42 used by carp (*Cyprinus carpio*) during steady swimming (Rome *et al.* 1988). However, some caution should be exercised in the interpretation of V/V_{max} ratios as the peak velocity used *in vivo* is often at the top end of the range or greater than would be predicted from steady-state force–velocity studies (Johnston *et*

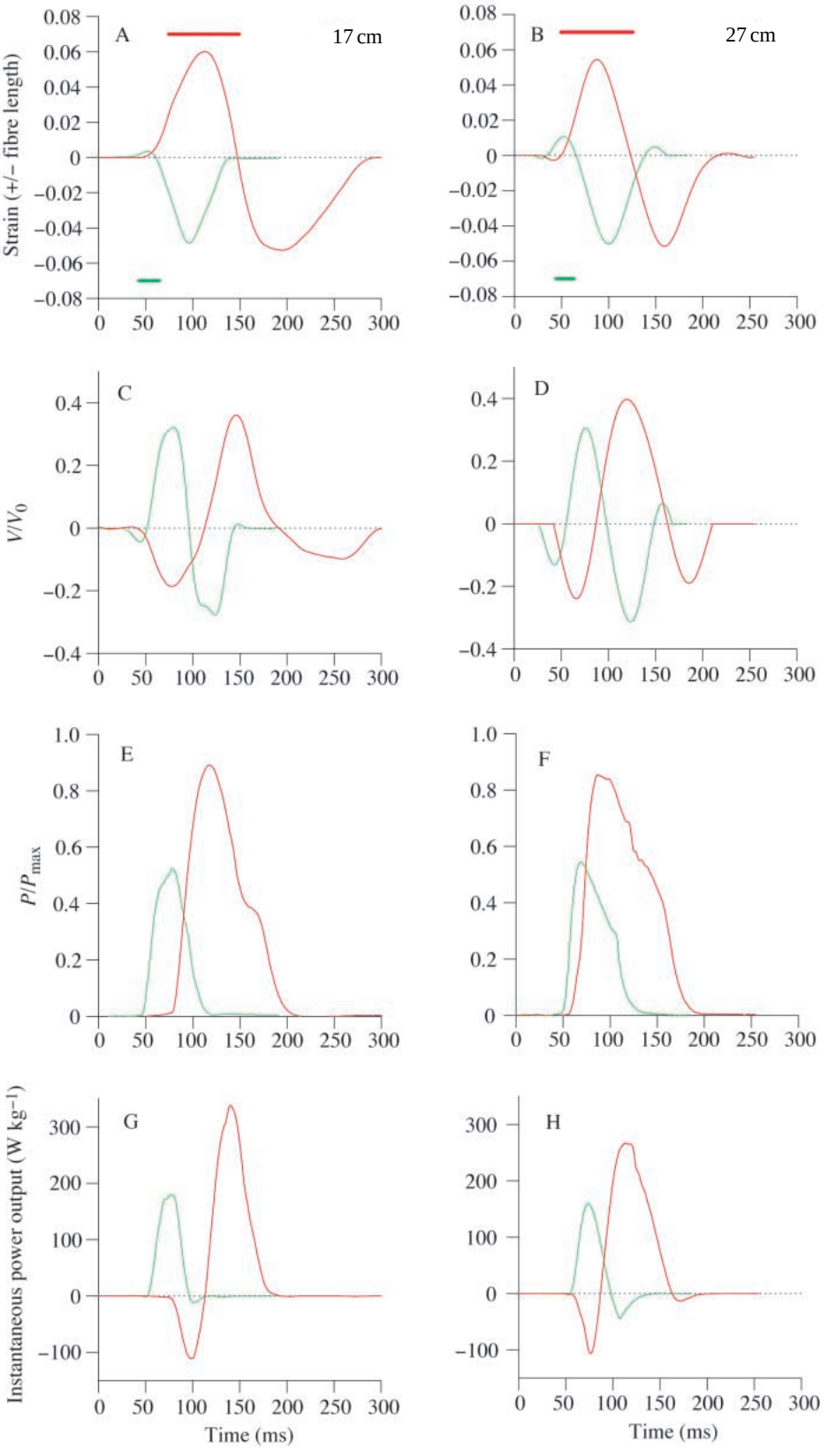

Fig. 6. Results from work-loop experiments using *in vivo* muscle length changes and activation patterns in fish of 17 cm and 27 cm total length. (A,B) Strain, where a strain of −0.05 depicts a 5% shortening of the muscle relative to the initial resting length. (C,D) Relative instantaneous shortening velocity (V/V_0, where V_0 is the unloaded shortening velocity) calculated by differentiating the instantaneous strain data. (E,F) Relative force P/P_{max}. P is the instantaneous force produced and P_{max} represents the maximum force determined under isometric conditions. (G,H) Instantaneous power output. Green and red traces refer to the C-bend and contralateral contraction, respectively. The straight lines in A and B represent stimulation durations.

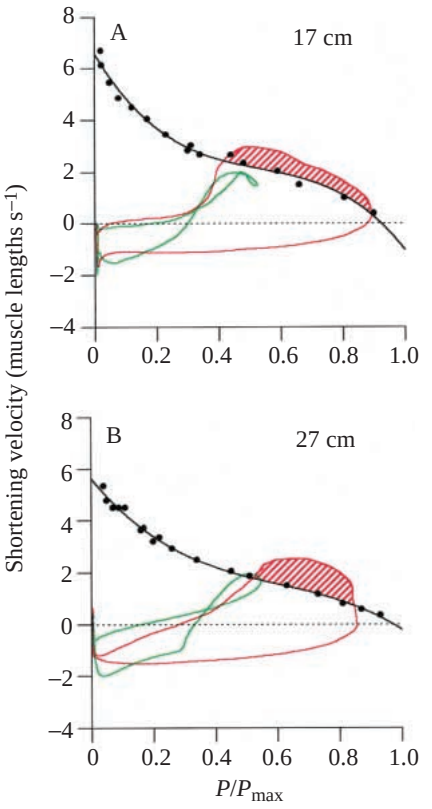

Fig. 7. Force–velocity curves derived from isovelocity shortening experiments (James *et al.* 1998) and work-loop experiments using the same fish muscle preparations used in Fig. 4. The solid black line represents a third-order polynomial fitted to the isovelocity data (filled circles) using a least-squares regression (r^2=0.993 and r^2=0.986 for the data from the 17 and 27 cm fish, respectively). Green and red traces represent the C-bend and the contralateral contraction, respectively. The shaded region represents the period where the performance under *in vivo* conditions exceeded that achieved during isovelocity contractions. Force (P) is expressed relative to P_{max}, the maximum force determined during isometric studies.

al. 1995; Franklin and Johnston, 1997). These studies have demonstrated that the V/V_{max} value used *in vivo* is affected by the degree of active pre-stretch, which in turn varies both along the length of the body and between the C-bend and the contralateral contraction. Therefore, V/V_{max} values provide an approximate but simplistic indication of the likely *in vivo* contractile performance of muscle.

Muscle performance during escape responses

The stress generated during the contralateral contraction approached and in a few fish actually exceeded that achieved during isometric contractions. Active muscle lengthening is known to enhance muscle force production, possibly by altering cross-bridge interactions with the thin filament (Edman *et al.* 1978). This force enhancement led to a significant increase in maximum instantaneous power output during the fast-start from the C-bend to the contralateral contraction. Therefore, muscle shortening during the C-bend is necessary to actively lengthen the contralateral muscle, such that the C-bend acts partially as a preparatory stroke enabling force enhancement to occur during the contralateral contraction. This can be equated to the findings on muscle power output during steady (Altringham *et al.* 1993) and unsteady (Johnston *et al.* 1993) swimming, where muscle shortening appears to travel in a wave from anterior to posterior to enable force enhancement to occur in all myotomes except those closest to the head of the fish.

The maximum instantaneous power outputs in this study exceeded those achieved by Johnston *et al.* (1995) for fast muscle from the same fish species at the higher temperature of 15 °C. They used strain waveforms calculated from the body position of the fish and measured muscle activation patterns obtained during escape responses. The probable reason for this discrepancy is the shorter period of stimulation during muscle lengthening used by Johnston *et al.* (1995), which would have resulted in lower levels of force enhancement.

Although the maximum instantaneous power output was higher during the contralateral contraction, 307 compared with 222 W kg^{-1} wet muscle mass, the mean power output over the abstracted cycle was not significantly different between the C-bend and the contralateral contraction. Mean power output for the abstracted cycle for the contralateral contraction and maximum instantaneous power output for both the C-bend and the contralateral contraction were all independent of body length. However, the mean power output for the abstracted cycle increased with body length for the C-bend, scaling as $L^{2.31}$, because strain was too low for maximum power output in the smaller fish. Although the intrinsic contractile properties of muscle change with body size (James *et al.* 1998), maximum instantaneous power output throughout the escape response and mean power output during the contralateral contraction remain relatively constant.

On the basis of hydrodynamic calculations and kinematic measurements, it has been suggested that the maximum mean muscle power output produced during the fast-start represents the limiting factor on performance (Frith and Blake, 1995; J. M. Wakeling and I. A. Johnston, unpublished results). In the present study, muscle fibres were found to produce close to their maximum power output, with individual optimisation of strain or stimulation parameters improving power output by mean values ranging from 2 to 20 %.

When instantaneous force and velocity values from the C-bend and contralateral contraction were plotted against the steady-state force–velocity relationship for the same muscles, power loops were produced which deviated from the steady-state curves (Fig. 7). The power loops demonstrate that under *in vivo* operating conditions muscle is generally unable to match the power output produced during *P–V* experiments (where muscle is maximally activated and shortens at a constant velocity). This is to be expected as in the animal the muscle needs time to activate, relax and re-lengthen to its original starting length (James *et al.* 1996). However, owing to force enhancement, the power loops produced under the

contralateral contraction conditions did exceed the *P–V* curve at higher values of P/P_{max}. The more active stretch the muscle received prior to shortening, the more the power loop exceeded the force–velocity curve, in agreement with the findings of Stevens (1993). However, under *in vivo* conditions, too much active stretch would compromise the mean power produced in the C-bend and the contralateral contraction.

The authors wish to thank Mr I. Johnston, Mr M. Coutts, Dr J. Wakeling and Dr C. Franklin for technical assistance. We would also like to thank Dr J. Wakeling for helpful discussion. This work was supported by a grant from the Biotechology and Biological Sciences Research Council of the U.K.

References

ALEXANDER, R. MCN. (1969). The orientation of muscle fibres in the myomeres of fishes. *J. mar. biol. Ass. U.K.* **49**, 263–290.

ALTRINGHAM, J. D. AND JOHNSTON, I. A. (1990). Scaling effects on muscle function: power output of isolated fish muscle fibres performing oscillatory work. *J. exp. Biol.* **151**, 453–467.

ALTRINGHAM, J. D., WARDLE, C. S. AND SMITH, C. I. (1993). Myotomal muscle function at different locations in the body of a swimming fish. *J. exp. Biol.* **182**, 191–206.

BAINBRIDGE, R. (1958). The speed of swimming of fish as related to size and to the frequency and amplitude of the tail beat. *J. exp. Biol.* **35**, 109–133.

CURTIN, N. A. AND WOLEDGE, R. C. (1988). Power output and force–velocity relationship of live fibres from white myotomal muscle of the dogfish *Scyliorhinus canicula*. *J. exp. Biol.* **140**, 187–197.

DOMENICI, P. AND BLAKE, R. W. (1997). The kinematics and performance of fish fast-start swimming. *J. exp. Biol.* **200**, 1165–1178.

EATON, R. C., BOMBARDIERI, R. A. AND MEYER, D. L. (1977). The Mauthner initiated startle response in teleost fish. *J. exp. Biol.* **66**, 65–81.

EDMAN, K. A. P., ELZINGA, G. AND NOBLE, M. I. M. (1978). Enhancement of mechanical performance by stretch during tetanic contractions of vertebrate skeletal muscle fibres. *J. Physiol., Lond.* **281**, 139–155.

FRANKLIN, C. E. AND JOHNSTON, I. A. (1997). Muscle power output during escape responses in an Antarctic fish. *J. exp. Biol.* **200**, 703–712.

FRITH, H. R. AND BLAKE, R. W. (1995). The mechanical power output and hydromechanical efficiency of northern pike (*Esox lucius*) fast-starts. *J. exp. Biol.* **198**, 1863–1873.

GIBSON, S. AND JOHNSTON, I. A. (1995). Scaling relationships, individual variation and the influence of temperature on maximum swimming speed in early settled stages of the turbot *Scopthalmus maximus*. *Mar. Biol.* **121**, 401–408.

JAMES, R. S., COLE, N. C., DAVIES, M. L. F. AND JOHNSTON, I. A. (1998). Scaling of intrinsic contractile properties and myofibrillar protein composition of fast muscle in the fish *Myoxocephalus scorpius* L. *J. exp. Biol.* **201**, 901–912.

JAMES, R. S., YOUNG, I. S., COX, V. M., GOLDSPINK, D. F. AND ALTRINGHAM, J. D. (1996). Isometric and isotonic muscle properties as determinants of work-loop muscle power output. *Pflügers Arch.* **432**, 767–774.

JAYNE, B. C. AND LAUDER, G. V. (1993). Red and white muscle activity and kinematics of the escape response of the bluegill sunfish during swimming. *J. comp. Physiol.* **173**, 495–508.

JAYNE, B. C. AND LAUDER, G. V. (1995). Are muscle fibres within myotomes activated synchronously? Patterns of recruitment within deep myomeric musculature during swimming in largemouth bass. *J. exp. Biol.* **198**, 805–815.

JOHNSTON, I. A., FRANKLIN, C. E. AND JOHNSON, T. P. (1993). Recruitment patterns and contractile properties of fast muscle fibres isolated from rostral and caudal myotomes of the short-horned sculpin. *J. exp. Biol.* **185**, 251–265.

JOHNSTON, I. A., VAN LEEUWEN, J. L., DAVIES, M. L. F. AND BEDDOW, T. (1995). How fish power predation fast starts. *J. exp. Biol.* **198**, 1851–1861.

JOSEPHSON, R. K. (1985). Mechanical power output from striated muscle during cyclic contraction. *J. exp. Biol.* **114**, 493–512.

KIRKPATRICK, S. E., COVELL, J. W. AND FRIEDMAN, W. F. (1973). A new technique for the continuous assessment of fetal and neonatal cardiac performance. *Am. J. Obstet. Gynecol.* **116**, 963–972.

LUTZ, G. J. AND ROME, L. C. (1994). Built for jumping: The design of the frog muscular system. *Science* **263**, 370–372.

ROME, L. C., FUNKE, R. P., ALEXANDER, R., MCN., LUTZ, G., ALDRIDGE, H., SCOTT, F. AND FREADMAN, M. (1988). Why animals have different muscle fibre types. *Nature* **335**, 824–827.

ROME, L. C. AND SOSNICKI, A. A. (1990). The influence of temperature on mechanics of red muscle in carp. *J. Physiol., Lond.* **427**, 151–169.

STEVENS, E. D. (1993). Relation between work and power calculated from force–velocity curves to that done during oscillatory work. *J. Muscle Res. Cell Motil.* **14**, 518–526.

TAMURA, Y. T., HATTA, I., MATSUDA, T., SUGI, H. AND TSUCHIYA, T. (1982). Changes in muscle stiffness during contraction recorded using ultrasonic waves. *Nature* **299**, 631–633.

TEMPLE, G. K. AND JOHNSTON, I. A. (1998). Testing hypotheses concerning the phenotypic plasticity of escape performance in fish of the family Cottidae. *J. exp. Biol.* **201**, 317–331.

VIDELER, J. J. AND WARDLE, C. S. (1991). Fish swimming stride by stride: speed limits and endurance. *Rev. Fish Biol. Fish.* **1**, 23–40.

WARDLE, C. S. (1980). Effect of temperature on the maximum swimming speeds of fishes. In *The Environmental Physiology of Fishes* (ed. M. A. Ali), pp. 519–531. New York: Plenum.

WARDLE, C. S., VIDELER, J. J. AND ALTRINGHAM, J. D. (1995). Tuning in to fish swimming waves: body form, swimming mode and muscle function. *J. exp. Biol.* **198**, 1629–1636.

WEBB, P. W. (1978). Fast-start performance and body form in seven species of teleost fish. *J. exp. Biol.* **74**, 211–226.

WEIHS, D. (1973). The mechanism of rapid starting of slender fish. *Biorheology* **10**, 343–350.

ZAR, J. H. (1984). *Biostatistical Analysis*. London: Prentice Hall International.